Deposition of hydrogen chloride gas on copper wafer depending on humidity and HCl concentration

Minh-Phuong Tran, Paola Gonzalez-Aguirre, Carlos Beitia, Jorgen Lundgren, Sung-In Moon, Hervé Fontaine

Energy transfer of Tb(tmhd)₃ - Rhodamine B in poly(methyl methacrylate) fiber for new photonic applications

P. Miluski[1]*, M. Kochanowicz[1], J. Zmojda[1], A. Baranowska[2], D. Dorosz[3]

[1] Faculty of Electrical Engineering, Bialystok University of Technology, Wiejska 45D, 15-351 Bialystok, Poland

[2] Faculty of Mechanical Engineering, Bialystok University of Technology, Wiejska 45C, 15-351 Bialystok, Poland

[3] Faculty of Materials Science and Ceramics, AGH University of Science and Technology, 30 Mickiewicza Av.,30-059 Krakow, Poland

corresponding author: *p.miluski@pb.edu.pl

Keywords: *organic luminescent dyes, lanthanides, Rhodamine B, energy transfer, FRET, polymer optical fiber*

Abstract. In our work we present the energy transfer phenomenon observed in poly(methyl methacrylate) co-doped by Tb(tmhd)₃ and Rhodamine B. The optical properties characterization (recorded luminescence spectra and decay time measurements) indicate efficient energy transfer (up to 67%) between used complexes. Additionally, the developed matrix was used for luminescent polymeric fiber fabrication. The co-doped PMMA fiber allows significant luminescence spectrum modification by using energy transfer and optical radiation reabsorption phenomena. Presented lanthanide-organic dye co-doped poly(methyl methacrylate) fiber can be used for new photonic applications of polymeric optical fibers.

1. Introduction

The luminescent properties of polymeric materials are attractive for numerous applications in optoelectronics. Nowadays, organic light-emissive compounds are intensively investigated for OLED (Organic Light Emitting Devices), fluorescent markers, illuminators, and sensors [1-12]. New luminescent properties can be obtained by using co-doping by lanthanides and organic dyes. Főrester Resonant Energy Transfer (FRET) between organic dyes has been intensively investigated for sensing applications. Super-resolution bioimaging and single molecule interactions are the most spectacular applications of organic dyes based FRET [13-16]. On the other hand, the lanthanide-based energy transfer is commonly used for effective excitation of rare earth ions for fiber lasers and upconversion emission [17-19]. The using of organic-inorganic dopants in the optical fiber structure imposes restrictions on properties of the optical host material. The simultaneous incorporation of lanthanides and organic dyes for optical fiber technology is possible by using polymeric host due to the low synthesis and thermoforming temperatures as well as various methods of doping with functional compounds (organic and inorganic) [20-23]. Also, doped polymers optical planar structures had found applications in new amplifiers constructions [24]. The several advantages of polymeric optical fibers such as: high elastic strain limits giving the ability to produce flexible optical fibers with significantly larger diameters (up to several mm), high numerical aperture, significantly lower manufacturing costs (extrusion and drawing processes are carried out temperatures below 300 °C) have been reported so far [25]. Among different polymeric materials, the poly(methyl methacrylate) (PMMA) is commonly used due to excellent optical properties and well-developed processing technology. High flexibility of poly(methyl methacrylate), wide doping possibility and biocompatibility can significantly extend the polymeric optical fibers applications fields [26, 27]. Among the functional organic compounds, the effective luminescence processes was reported in xanthene, oxazine, aminocoumarins dyes, and aromatic hydrocarbons

[28-33]. Typically they are characterized by broad bands of excitation and emission spectra resulting from the partial disappearance of the oscillation structure as a result of interactions between the fluorophores and the surrounding medium. Most of the organic dyes are also characterized by a short luminescence time of nanoseconds [28]. Lanthanides, thanks to well-defined emission bands, long decay times, have found wide application in the construction of wavelength converters, laser systems, sensors, optical amplifiers and radiation sources [34-39]. The electrons in the 4f shell of lanthanides are shielded from the surroundings by the filled 5s and 5p states [40]. Due to the small influence of the matrix on the optical transitions within the 4f shell, the narrow absorption and emission bands occur. The effective excitation of rare earth ions requires well spectrally fitted sources with high power density (e.g. laser diodes). In polymeric materials, increasing the cross-section of absorption is possible by using organometallic lanthanide compounds. The broad absorption spectrum of ligand enables effective transfer of absorbed energy to the rare earth ion by using energy transfer antenna effect. Moreover, its shielding properties limit the possibility of nonradiative transition and luminescence quenching by polymeric matrix and obtaining the decay times an order of ms [41]. The compositions of lanthanides and organic dyes, due to their significantly different optical properties, can be used for fabrication of new functional optical polymers. One of the most interesting phenomenon for luminescence spectrum modifications in optical fibers is energy transfer between rare earth ions and organic dyes. The article presents the FRET phenomenon investigation for Terbium(III)-tris-(2,2,6,6-tetramethyl-3,5-heptanedionate) $(Tb(tmhd)_3)$ and Rhodamine B (RhB) in poly(methyl methacrylate) matrix.

2. Theory of FRET

The energy transfer theory was reported in literature [42-47]. The FRET between molecules of donor D $(Tb(tmhd)_3)$ and acceptor A (RhB) is obtaining according to equation:

$$D' + A \rightarrow D + A' \qquad (1)$$

$$A' \rightarrow A + h\nu \qquad (2)$$

According to Förster theory the rate of energy transfer for is described by:

$$k_T(r) = \frac{Q_D \kappa^2}{\tau_D r^6} \left(\frac{9000(ln10)}{128\pi^5 Nn^4} \right) \int_0^\infty F_D(\lambda)\, \varepsilon_A(\lambda) \lambda^4 d\lambda = \frac{1}{\tau_D} \left(\frac{R_0}{r} \right)^6 \qquad (3)$$

where: r – distance between donor and acceptor molecules, Q_D – quantum yield of donor in the absence of acceptor, n – refractive index of medium, N is Avogadro's number, τ_D is the lifetime of the donor in the absence of acceptor; $F_D(\lambda)$ is the fluorescence intensity of the donor in the wavelength range λ to $\lambda + \Delta\lambda$, with the total intensity normalized to 1, $\varepsilon_A(\lambda)$ is the extinction coefficient of the acceptor and R_0 called Förster distance in Å:

$$R_0^6 = \frac{9000(ln10)Q_D \kappa^2}{128\pi^5 Nn^4} \int_0^\infty F_D(\lambda)\, \varepsilon_A(\lambda) \lambda^4 d\lambda \approx 9.78 \cdot 10^3 [\kappa^2 n^{-4} Q_D J(\lambda)]^{\frac{1}{6}} \qquad (4)$$

R_0 is distance when 50% of energy transfer efficiency occurs. The $J(\lambda)$ is a degree of spectral overlap between the donor emission and the acceptor absorption (Fig. 1a):

$$J(\lambda) = \frac{\int_0^\infty F_D(\lambda)\varepsilon_A(\lambda)\lambda^4 d\lambda}{\int_0^\infty F_D(\lambda)d\lambda} \qquad (5)$$

The efficiency of energy transfer is the ratio of the transfer rate to the total decay rate of the donor and can be expressed using the equation:

$$E = 1 - \frac{F_{DA}}{F_D} \qquad (6)$$

or

$$E = 1 - \frac{\tau_{DA}}{\tau_D} \qquad (7)$$

where: F_{DA} and F_D is the luminescence intensity of the donor in the presence and absence of acceptor respectively, and accordingly τ_{DA} and τ_D is decay time of the donor in the presence and absence of acceptor.
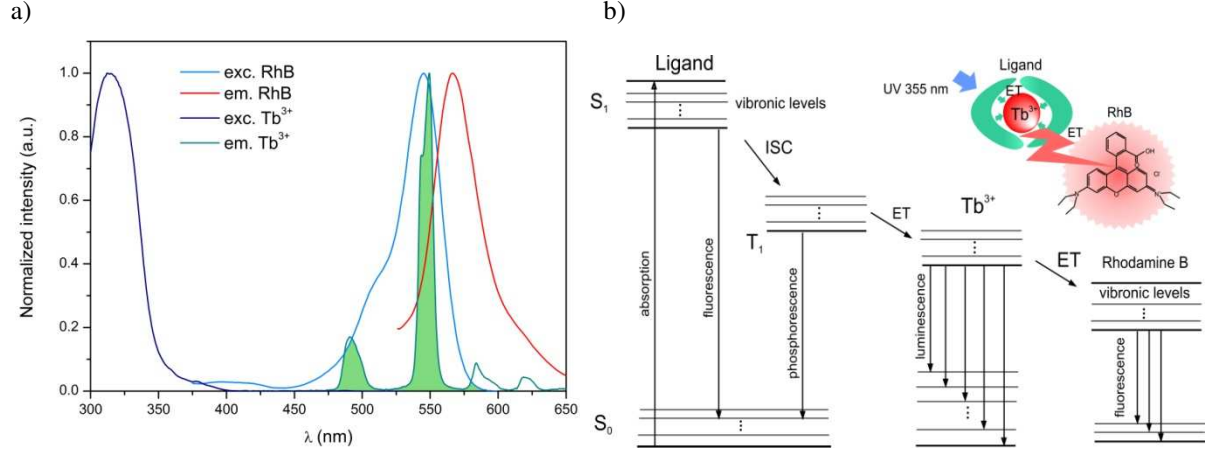
a)

b)

Fig. 1. a) Normalized absorption/emission spectra of Tb(tmhd)$_3$ and Rhodamine B, b) The energy transfer scheme of Tb(tmhd)$_3$ to Rhodamine B.

Assuming the FRET efficiency depends on the quantum emission efficiency of the donor in absorption region of the acceptor, donor and acceptor emission and absorption spectrum overlap integral and the distance between energy exchanging molecules. Proposed energy transfer mechanism is presented in Fig.1b.

3.   Research methodology

The specimens were fabricated in Bialystok University of Technology laboratory. The methyl methacrylate (MMA), Benzoyl Peroxide (BP), Rhodamine B, and Terbium(III)-tris-(2,2,6,6-tetramethyl-3,5-heptanedionate) (Tb(tmhd)$_3$) were supplied by Sigma-Aldrich with standard >99% purity. The chemicals were used without additional purification except for MMA (stabilizer agent has been removed before polymerization). The specimens and polymeric fiber preforms were polymerized at 30 h at 65-80 °C. The used lanthanide (Tb(tmhd)$_3$) and organic dye (RhB) doping process were performed directly during PMMA polymerization. The terbium ions concentration was constant while RhB varies to obtain several energy transfer rates (Tab. 1).

Table 1. The concentrations of Tb(tmhd)$_3$ - RhB used in experiment

No.	Tb(tmhd)$_3$ molar concentration $\cdot 10^{-3}$	Rhodamine B molar concentration $\cdot 10^{-6}$
1	1.57	0.00
2	1.58	0.48
3	1.58	0.84
4	1.56	1.04
5	1.57	1.34

Uniform distribution of dopants with no PMMA defects were observed in the fabricated specimens. PMMA specimens were prepared by cutting (10 mm diameter preform) into 2.8 mm thick discs and polishing. The characterized fiber was fabricated using optical fiber drawing tower (furnace temperatures T=170-200 °C, preform feeding 0.5 cm/min, drawing speed 20-32 cm/min, complexes concentrations: pos. 5 in Tab. 1). The fibers diameters range 0.4 – 2.1 mm were produced. The fiber diameter chosen for characterization was 1.8 mm since glass transition temperature of PMMA is c.a. 105 °C and low excitation laser power density is required. The well known cut-back method was used for photoluminescence spectra recording in fiber structure. Additionally, the collimator lens was used for efficient coupling of laser radiation into the fiber. The spectra were recorded using Stellarnet Green Wave spectrometer (300-900 nm). The absorption spectra of bulk specimens were measured using deuterium halogen Stellarnet SL5 lamp (UV+VIS). The luminescence spectra and lifetime measurements were performed using Q-switched laser systems Continuum Minilite1 (third harmonic 355 nm) and Acton Spectra Pro 2300i monochromator. All measurements have been performed at temperature 20 °C.

4. Results

The Tb^{3+} doped PMMA properties were investigated so far [48]. A colorless and mild red color was observed for samples $Tb(tmhd)_3$ and $Tb(tmhd)_3$-RhB, respectively. The Rhodamine B absorption band with a maximum at 530 nm can be noticed for $Tb(tmhd)_3$-RhB specimen (Fig. 2a) which is in good agreement with literature data [49, 50]. The absorption edge below 350 nm confirms effective excitation possibility by using third harmonic (355 nm) of Nd:YAG laser.
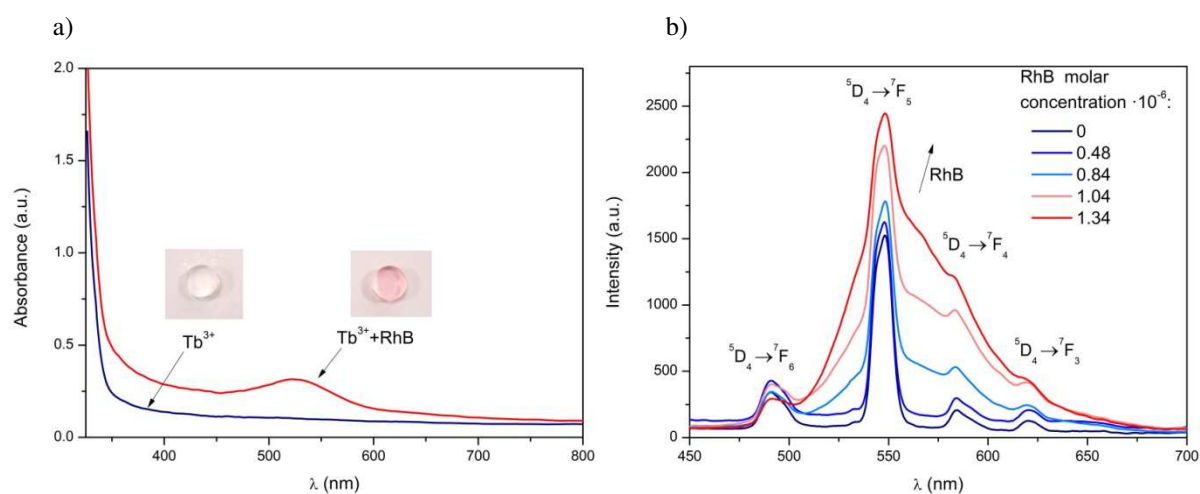

Fig. 2. The Tb^{3+}- RhB doped PMMA optical measurements: a) absorbance spectra measured for specimens no. 1 and 5, b) emission spectra at excitation 355 nm.

The luminescence spectra of fabricated specimens for RhB molar concentration range $0-1.34 \cdot 10^{-6}$ are presented in Fig. 2b. The luminescence of terbium ions due to the fact of polymeric host is limited to high-intensity peaks $^5D_4 \rightarrow ^7F_6$ (486 nm), $^5D_4 \rightarrow ^7F_5$ (548 nm), $^5D_4 \rightarrow ^7F_4$ (583 nm), $^5D_4 \rightarrow ^7F_3$ (622 nm). The recorded spectra are in good agreement with those reported in aqueous solution and glasses [41, 43, 44]. The hypersensitivity of the $^5D_4$ $\rightarrow ^7F_6$ terbium transition can be used for lanthanide environment characterization. The antenna effect in $Tb(tmhd)_3$ complex causes that no broadband fluorescence peak can be observed in the recorded spectrum (effective energy transfer from ligand triplet state to $^5D_4$ of terbium). The single state S_1 can also directly transfer

the energy to higher energy levels of the lanthanide ion and next to the $^5D_4$ level by non-radiative relaxations. The well known Rhodamine B fluorescence spectrum with its maximum c.a. 550 nm is noticeable in recorded spectra (Fig. 2b). The luminescence decay curve was measured at 355 nm excitation and $^5D_4 \rightarrow ^7F_5$ transition monitoring (Fig. 3a). The double exponential phase decay curve (adjusted R-squared above 0.98 for all calculated curves) can be used for decay character estimation [51]:

$$I(t) = A_1 \exp\left(-\frac{t}{\tau_1}\right) + A_2 \exp\left(-\frac{t}{\tau_2}\right) \tag{8}$$

where:

A_1 and A_2 are the amplitudes, and τ_1 and τ_2 are the rate constants of decay respectively of the two exponentials. The average decay time constant (τ_{avg}) was calculated using:

$$\langle \tau_{avg} \rangle = \frac{A_1 \tau_1^2 + A_2 \tau_2^2}{A_1 \tau_1 + A_2 \tau_2} \tag{9}$$

The character of bi-exponential shape observed also for single dopant Tb(tmhd)$_3$ suggest the dynamic quenching by terbium ions concentration (existence of the strong Tb–Tb interaction and energy exchange in the solid state matrix) [52]. An intense luminescence and relatively long measured decay time of Tb(tmhd)$_3$ equals 0.42 ms ($^5D_4$) confirms that used terbium complex can be successfully used for PMMA doping [40, 41]. The energy transfer from trivalent terbium to Rhodamine B is noticeable by shortening of terbium ions decay time and changing the luminescence spectrum (the intensity of terbium luminescence content decrease vs. RhB concentration).

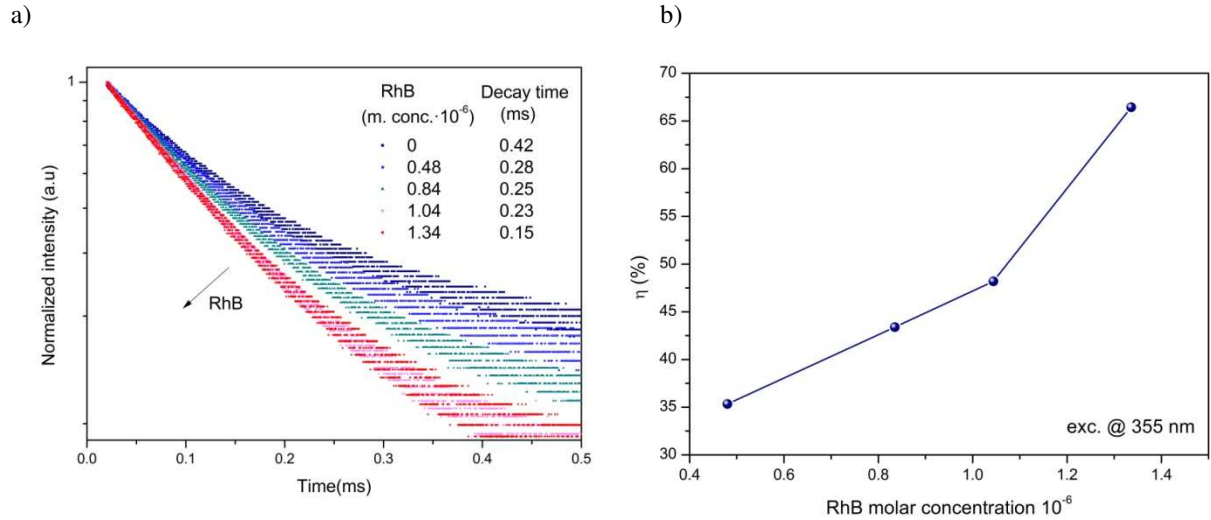a)   b)

Fig. 3. a) The luminescence decay time curve at exc. 355 nm, monitoring at 542 nm, b) The FRET efficiency vs. RhB concentration.

The energy transfer efficiency was calculated using decay time measurements using equation 7. Calculated the high efficiency of energy transfer observed for low RhB concentration is related to high absorption cross section of Rhodamine B (max σ_a=3.4·10^{-20} m^2) [53]. In such circumstances, much lower RhB concentration (maximum used RhB molar concentration 1.34·10^{-6}, c.a. 1000 times less than Tb(tmhd)$_3$ significantly change the energy transfer efficiency). This phenomenon is one of the advantages of using lanthanide markers for fluorescence-based FRET microscopy since extremely low acceptor concentration can be detected using this technique [13-16]. The obtained results show that the energy transfer efficiency from 35.2 to 67.0 % can be obtained by

changing the RhB molar concentration 0.48-1.34·10^{-6}. The lanthanides and organic dyes in polymeric optical fibers offer different luminescence spectrum modification possibility. The large Stokes shift which is characteristic for trivalent lanthanide ions (typically above 150 nm) [44] causes the spectral attenuation of polymeric fiber is dominant for changes observed in luminescence spectrum. No maximum emission bands shift vs. fiber length can be observed. The Tb^{3+} and Eu^{3+} doped PMMA fiber were previously investigated by the authors [48, 54, 55]. On the other hand, overlapping of absorption and emission spectra in organic fluorophores causes efficient reabsorption of radiation propagating in the polymeric fiber. In such circumstances, significant typically red shift direction is observed in organic dyes doped polymeric fibers [56]. Measured spectra in $Tb(tmhd)_3$-RhB doped fiber are presented in Fig. 4a.
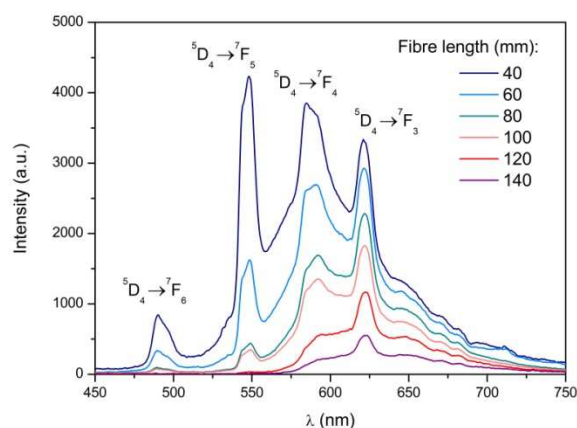
a) b)
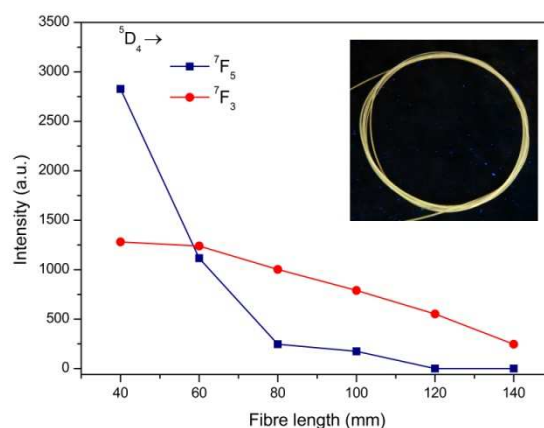

Fig. 4. a) The luminescence spectra for several fiber lengths at exc. 355 nm, b) The intensity of $^5D_4 \rightarrow {}^7F_5$ (548 nm) and $^5D_4 \rightarrow {}^7F_3$ (622 nm) vs. fiber length, inset: $Tb(tmhd)_3$-RhB doped fiber under 365 nm excitation (mercury vapor black light).

The recorded spectra (Fig. 4a) are the composition of characteristic terbium (identified transitions marked on the graph) and Rhodamine B (wide emission band). No spectrum shift can be observed for the terbium luminescence spectrum according to large Stokes shift. The emission bands which correspond to $^5D_4 \rightarrow {}^7F_6$ (486 nm), $^5D_4 \rightarrow {}^7F_5$ (548 nm), $^5D_4 \rightarrow {}^7F_4$ (583 nm) are strongly absorbed in the fabricated fiber structure according to the high overlapping integral of emission terbium and absorption of Rhodamine B (Fig. 1a). Additionally, red shift is observed for RhB luminescence. The maximum of its emission was identified as 560 nm for thin specimens and 590-620 nm for fiber length 40-140 mm respectively. The comparison of $^5D_4 \rightarrow {}^7F_5$ (548 nm) and $^5D_4 \rightarrow {}^7F_3$ (622 nm) intensity emission bands vs. fiber length are shown in Fig. 4b. The most insensitive terbium emission band at 548 nm ($^5D_4 \rightarrow {}^7F_5$) is fully absorbed for fiber length 120 mm in opposite to 622 nm ($^5D_4 \rightarrow {}^7F_3$) which can be observed in the luminescence spectrum for longer distances. Additionally, the chromaticity coordinates CIE 1931 were calculated and presented in Fig. 5. Presented results show luminescence color modification from amber (l=40 mm, x=0.50, y=0.47) to red (l=140 mm, x=0.64, y=0.35) and potential applications in lightening technology.
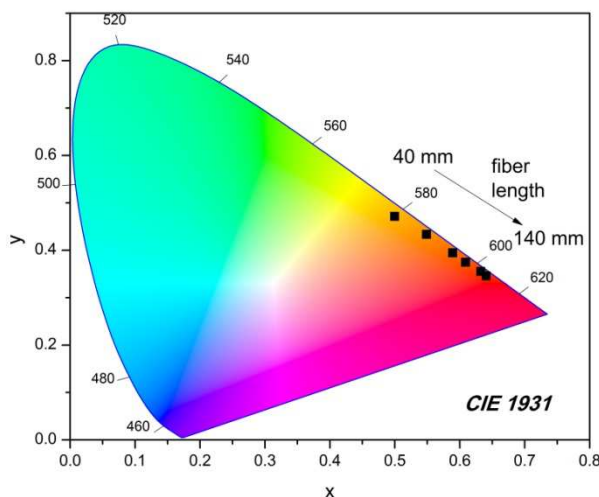
Fig. 5. The chromaticity coordinates of Tb3+- RhB doped PMMA fiber, exc. 355 nm.

The Tb(tmhd)$_3$-RhB energy transfer and reabsorption process can be used for luminescence spectrum modification in the cylindrical structure of poly(methyl methacrylate) fiber. The compositions of lanthanides and fluorophores, due to their optical properties, different mechanisms of luminescence spectra modification in optical fibers, and energy transfer between rare earth ions and organic dyes can be used for obtaining new luminescent properties of polymeric optical fibers.

5.   Summary

The fabrication and optical properties characterization of PMMA co-doped by Tb(tmhd)$_3$-RhB. The recorded luminescence spectra and decay time of terbium-Rhodamine B co-doped specimens confirm FRET mechanism between used complexes. The energy transfer has been characterized in terms of RhB molar concentration range 0-1.34·10^{-6}. The maximum energy transfer efficiency 67% was observed for highest used RhB concentration. The Tb(tmhd)$_3$-RhB co-doped PMMA fiber shown significant luminescence spectrum modification resulting from energy transfer and reabsorption phenomena. Presented properties of lanthanide-organic dye co-doped PMMA can be used for developing new applications in optical fiber technology (e.g. amplifiers, lasers, sensors).

References

[1]   N. Gahlaut, L.W. Miller, Time-resolved microscopy for imaging lanthanide luminescence in living cells, Cytometry A 77(12) (2010) 1113–1125.

[2]   F. Tauro, M. Aureli, M. Porfiri, S. Grimaldi, Characterization of buoyant fluorescent particles for field observations of water flows, Sensors 10(12) (2010) 11512-11529.

[3]   W.W. Yua, E. Chang, R. Drezek, V.L. Colvin, Water-soluble quantum dots or biomedical applications, Biochemical and Biophysical Research Communications 348 (3) (2006) 781–786.

[4]   O. Korostynska, K. Arshak, E. Gill, A. Arshak, Review on state-of-the-art in polymer based pH sensors, Sensors 7 (2007) 3027–3042.

[5]   P. Miluski, D. Dorosz, M. Kochanowicz, J. Zmojda, Fluorescent polymeric optical fibre illuminator, Electronics Letters 52(18) (2016) 1550 – 1552.

[6]   L. Bilro, N. Alberto, J.L. Pinto , R. Nogueira, Optical sensors based on plastic fibers, Sensors 12(9) (2012) 12184.

[7]   C. Baleizao, S. Nagl, M. Schaferling, M.N. Berberan-Santos, O.S. Wolfbeis, Dual fluorescence sensor for trace oxygen and temperature with unmatched range and sensitivity, Analytical Chemistry 80 (2008) 6449

[8]   P. Miluski, D. Dorosz, M. Kochanowicz, J. Zmojda, Optical fibre temperature sensor based on fluorescein and rhodamine codoped polymer layer, Proc. of SPIE (2013) 8903 89030C-6.

[9]   J. Arrue, F. Jiménez, I. Ayesta, M. Asunción Illarramendi, J. Zubia, Polymer-optical-fiber lasers and amplifiers doped with organic dyes, Polymers 3 (2011) 1162–1180.

[10] G. Williams, C. Backhouse, H. Aziz, Integration of organic light emitting diodes and organic photodetectors for lab-on-a-chip bio-detection systems, Electronics 3 (2014) 43–75.

[11] G. Zissis, P. Bertoldi, 2014 Status report on organic light emitting diodes (OLED), Eur. Comm. Jt. Res. Cent. (2014).

[12] Ł. Dziuda, Fiber-optic sensors for monitoring patient physiological parameters: a review of applicable technologies and relevance to use during magnetic resonance imaging procedures, Journal of Biomedical Optics 20(1) (2015) 010901.

[13]   T. Ha, Single-molecule Fluorescence Resonance Energy Transfer, Methods 25 (2001) 78–86.

[14]   D.K. Sasmal, L. Pulido, S. Kasal, J. Huang, Single-molecule Fluorescence Resonance Energy Transfer in molecular biology, Nanoscale 8 (2016) 19928-19944.

[15] A.T. Brunger, P. Strop, M. Vrljic, S. Chu, K.R. Weninger, Three-dimensional molecular modeling with single molecule FRET, Journal of Structural Biology 173 (2011) 497–505.

[16] S.J. Holden, S. Uphoff, J. Hohlbein, D. Yadin, L. Le Reste, O.J. Britton, A.N. Kapanidis, Defining the limits of single-molecule FRET resolution in TIRF microscopy, Biophysical Journal 99 (2010) 3102–3111.

[17] H. Dong, L.-D. Sun, C.-H. Yan, Energy transfer in lanthanide upconversion studies for extended optical applications, Chem. Soc. Rev. 44 (2015) 1608-1634.

[18] A. Zając, D. Dorosz, M. Kochanowicz, M. Skórczakowski, J. Świderski, Fibre lasers – conditioning constructional and technological, Bulletin of the Polish Academy of Sciences Technical Sciences 58(4) (2010) 491-502.

[19] M.C. Falconi, D. Laneve, F. Prudenzano, Advances in Mid-IR fiber lasers: tellurite, fluoride and chalcogenide, Fibers 5 (2017) 23.

[20]   G. Hebbink, Luminescent materials based on lanthanide ions, Twente University Press (2002) ISBN 9036517869

[21] P. Miluski, Luminescent properties of Oxazine 170 Perchlorate doped PMMA fiber, Fibers 5(2) (2017) 15.

[22] J. Sarnecki, G. Gawlik, L. Lipińska, O. Jeremiasz, Polymer luminescent concentrators containing oxide nanocrystals doped with rare-earth elements matched to an edge-illuminated silicon solar cell, Electronic Materials 43(4) (2015) 10-17.

[23] P. Polis, A.M. Jusza, K.P. Anders, A. Jastrzębska, A. Olszyna, J. Jureczko, W. Fabianowski, A. Kunicki, R. Piramidowicz, Synthesis and characterization of $RE^{3+}:Al_2O_3$ nanopowders for application in the polymer based composite light sources, Proc. of SPIE 8435 (2012) 84352A-1.

[24] K. Yamashita, H. Taniguchi, S. Yuyama, K. Oe, Continuous-wave stimulated emission and optical amplification in europium (III)-aluminum nanocluster-doped polymeric waveguide, Applied Physics Letters 91 (2007) 081115.

[25] K. Peters, Polymer optical fiber sensors—a review, Smart Mater. Struct. 20 (2011) 013002.

[26] B. Selm, E.A. Gűrel, M. Rothmaier, R.M. Rossi, L.J. Scherer, Polymeric optical fiber fabrics for illumination and sensorial applications in textiles, Journal of Intelligent Material Systems and Structures, 21 (2010) 1061-1071.

[27] U.H.P. Fischer, M. Haupt, M. Joncic, Optical transmission systems using polymeric fibers, Optoelectronics - Devices and Applications, book edited by Padmanabhan Predeep (2011) ISBN 978-953-307-576-1.

[28] K.H. Drexhage, Fluorescence efficiency of laser dyes, Journal of Research of the National Bureau of Standards-A. Physics and Chemistry 3 (1976) 421-428.

[29] A.H. Al-Hamdani, A.S. Al-Ethawi, R. Al-Hamdani, Fluorescence efficiency of Rhodamine 6G Doped PMMA, Journal of Materials Science and Engineering 4(12) (2010) 57-61.

[30] M. Kakuichi, K. Kasatani, Y. Morita, H. Okamoto, J. Kawamata, Fluorescent nanoparticles of Anthracene and bis-MSB, Nano Studies 7 (2013) 177-184.

[31] A. Köhler, H. Bässler, Triplet states in organic semiconductors, Materials Science and Engineering R 66 (2009) 71–109.

[32] M.R.M. Izawa, D.M. Applin, L. Norman, E.A. Cloutis, Reflectance spectroscopy (350–2500 nm) of solid-state polycyclic aromatic hydrocarbons (PAHs), Icarus 237 (2014) 159–181.

[33] M. Zyskowski, P. Miluski, J. Zmojda, M. Kochanowicz, Measurement and analysis of absolute quantum yield of Rhodamine B doped PMMA, Proc. of SPIE 10031 (2016) 100310K-1.

[34] M.E. Fermann, A. Galvanauskas, G. Sucha, D. Harter, Fiber lasers for ultrafast optics, Appl. Phys. B 65(2) (1997) 259–275.

[35] J. Kim, D.B.S. Soh, J. Nilsson, D.J. Richardson, J.K. Sahu, Fiber design for high-power low-cost Yb:Al-doped fiber laser operating at 980 nm, IEEE Journal of Selected Topics in Quantum Electronics, 13(3) (2007) 588- 597.

[36] J. Zmojda , M. Kochanowicz, P. Miluski, D. Dorosz, Side-detecting optical fiber doped with Tb^{3+} for ultraviolet sensor application, Fibers 2 (2014) 150–157.

[37] E. Desurvire, J.R. Simpson, Amplification of spontaneous emission in Erbium-doped single-mode fibers, J. Lightwave Tech. 7(5) (1989) 835-845.

[38] P.C. Becker, N.A. Olsson, J.R. Simpson, Erbium-doped fiber amplifiers: fundamentals and technology, Academic Press, San Diego (1999)

[39] D. Dorosz, J. Dorosz, A. Zając, J. Zmojda, M. Kochanowicz, Active optical fibres for application in laser and broadband ASE sources, Bulletin of the Polish Academy of Sciences, Technical Sciences 60(4) (2012) 673-682.

[40] M.H.V. Werts, Making sense of lanthanide luminescence, Science Progress 88(2) (2005) 101–131.

[41] K. Binnemans, Lanthanide-based luminescent hybrid materials, Chem. Rev. 109 (2009) 4283–4374.

[42] M.-C. Chirio-Lebrun, M. Prats, Fluorescence resonance energy transfer (FRET): theory and experiments, Biochcfnical Education 26 (1998) 320-323.

[43] P.R. Selvin, Lanthanide-based resonance energy transfer, IEEE Journal of Selected Topics in Quantum Electronics 2(4) (1997) 1077-1087.

[44] M. Xiao, P.R. Selvin, Quantum yields of luminescent lanthanide chelates and far-red dyes measured by resonance energy transfer, J. Am. Chem. Soc. 123 (2001) 7067-7073.

[45] P.R Selvin, J.E. Hearst, Luminescence energy transfer using a terbium chelate: improvements on fluorescence energy transfer, Proc Natl Acad Sci U S A. 91 (21) (1994) 10024-10028.

[46] D. Seth, D. Chakrabarty, A. Chakraborty, N. Sarkar, Study of energy transfer from 7-amino coumarin donors to rhodamine 6G acceptor in non-aqueous reverse micelles, Chemical Physics Letters 401 (2005) 546–552.

[47] N. Hildebrandt, K. D. Wegner, W.R. Algar, Luminescent terbium complexes: Superior Förster resonance energy transfer donors for flexible and sensitive multiplexed biosensing, Coordination Chemistry Reviews 273–274 (2014) 125-138.

[48] P. Miluski, M. Kochanowicz, J. Zmojda, D. Dorosz, Luminescent properties of Tb^{3+}-doped poly(methyl methacrylate) fiber, Chinese Optics Letters 15(7) (2017) 070602.

[49] C. Núñez, M. Diniz, A.A. Dos Santos, J.L. Capelo, C. Lodeiro, New rhodamine dimer probes for mercury detection via color changes and enhancement of the fluorescence emission: Fast recognition in cellulose supported devices, Dyes and Pigments 101 (2014) 156-163.

[50] M. Fikry, M.M. Omar, L.Z. Ismail, Effect of host medium on the fluorescence emission intensity of Rhodamine B in liquid and solid phase, J Fluoresc 19 (2009) 741–746.

[51] W. Chen, R. Fan, H. Zhang, Y. Dong, P. Wanga, Y. Yang, Tunable white-light emission PMMA-supported film materials containing lanthanide coordination polymers: preparation, characterization, and properties, Dalton Trans. 46(13) (2017) 4265-4277.

[52] H.-J. Zhang, R.-Q. Fan, X.-M. Wang, P. Wang, Y.-L. Wang, Y.-L. Yang, Preparation, characterization, and properties of PMMA-doped polymer film materials: a study on the effect of terbium ions on luminescence and lifetime enhancement, Dalton Trans. 44 (2015) 2871-2879.

[53] A. Tagaya, S. Teramoto, T. Yamamoto, K. Fuji, E. Nihei, Y. Koike, K. Sasaki, Theoretical and experimental investigation of rhodamine B-doped polymer optical fiber amplifiers, IEEE Journal of Quantum Electronics 31(12) (1995) 2215–2220.

[54] P. Miluski, M. Kochanowicz, J. Zmojda, D. Dorosz, The properties of Eu3+ doped poly(methyl methacrylate) optical fibre, Optical Engineering 56(2) (2017) 027106.

[55] P. Miluski, M. Kochanowicz, J. Zmojda, D. Dorosz, Multicolor emission of Tb3+/Eu3+ co-doped poly(methyl methacrylate) for optical fibre technology, Photonics Letters of Poland 9(4) (2017) 110–112.

[56] H. Liang, Z. Zheng, Z. Li, J. Xu, B. Chen, H. Zhao, Q. Zhang, H. Ming, Fabrication and amplification of Rhodamine B-doped step-index polymer optical fiber, Journal of Applied Polymer Science 93(2) (2004) 681–685.

[57] P. Miluski, M. Kochanowicz, J. Zmojda, D. Dorosz, Luminescent polymer optical fibre sensor for temperature measurement, Acta Physica Polonica Series A 127(3) (2015) 730-733.

[58] P. Miluski, M. Kochanowicz, J. Zmojda, D. Dorosz, Energy conversion in 7-(Diethylamino)coumarin doped PMMA fluorescent fibre, Optical and Quantum Electronics 49(132) (2017), https://doi.org/10.1007/s11082-017-0971-1.

[59] P. Miluski, Luminescent properties of Oxazine 170 Perchlorate doped PMMA fiber, Fibers 5(2) (2017) 15.

[60] Z. Zhiqiang, L. Hao, M. Hai, Z. Qijin, Y. Yuanqin, L. Shilin, Z. Yunsheng, X. Jianping, Rhodamine 6G-doped polymer optical fiber amplifiers, Chinese Optics Letters 2 (2004) 67–68.

[61] M. Sheeba, M. Rajesh, V. P. N. Nampoorj, P. Radhakrishnan, Fabrication and characterization of dye mixture doped polymer optical fiber as a broad wavelength optical amplifier, Applied Optics 47(11) (2008) 884–889.

[62] P. Miluski, M. Kochanowicz, J. Zmojda, D. Dorosz, 1,4-Bis(2-methylstyryl)benzene doped PMMA fibre for blue range fluorescent applications, Spectrochimica Acta Part A: Molecular and Biomolecular Spectroscopy 192 (2017) 88-92.

[63] P. Miluski, M. Kochanowicz, J. Zmojda, D. Dorosz, Emission properties and energy transfer in Perylene-Rhodamine 6 G co-doped polymeric fiber, Chinese Optics Letters 14(12) (2016) 121602–121607.

Figures captions:

Fig. 1. a) Normalized absorption/emission spectra of Tb(tmhd)$_3$ and Rhodamine B, b) The energy transfer scheme of Tb(tmhd)$_3$ to Rhodamine B.

Fig. 2. Fig. 2. The Tb^{3+}- RhB doped PMMA optical measurements: a) absorbance spectra measured for specimens no. 1 and 5, b) emission spectra at excitation 355 nm.

Fig. 3. a) The luminescence decay time curve at exc. 355 nm, monitoring at 542 nm, b) The FRET efficiency vs. RhB concentration.

Fig. 4. a) The luminescence spectra for several fiber lengths at exc. 355 nm, b) The intensity of $^5D_4 \rightarrow ^7F_5$ (548 nm) and $^5D_4 \rightarrow ^7F_3$ (622 nm) vs. fiber length, inset: Tb(tmhd)$_3$-RhB doped fiber under 365 nm excitation (mercury vapor black light).

Table 1. The concentrations of Tb(tmhd)$_3$ - RhB used in experiment